

# CO Oxidation on Supported Nano-Au Catalysts Synthesized from a $[\text{Au}_6(\text{PPh}_3)_6](\text{BF}_4)_2$ Complex

T. V. Choudhary,\* C. Sivadinarayana,\* C. C. Chusuei,\*<sup>1</sup> A. K. Datye,† J. P. Fackler, Jr.,\* and D. W. Goodman\*,<sup>2</sup>

\*Chemistry Department, Texas A&M University, College Station, Texas 77842-3012; and †Chemical Engineering Department, University of New Mexico, Albuquerque, New Mexico 87131

Received July 16, 2001; revised December 4, 2001; accepted January 15, 2002

Highly active and stable nano-Au catalysts have been synthesized by the interaction of an Au cluster–phosphine complex with a  $\text{TiO}_2$  support. These catalysts have been characterized by transmission electron microscopy, X-ray photoelectron spectroscopy and tested for CO oxidation. The pretreatment conditions had a profound influence on the CO oxidation activity of the Au/ $\text{TiO}_2$  catalysts. Under optimum pretreatment conditions these catalysts showed high catalytic activity. This is noteworthy, considering that previous studies (Y. Yuan, A. P. Kozlova, K. Akasura, H. Wan, K. Tsai, and Y. Iwasawa, *J. Catal.* (1997) 170, 191) on similar systems (different pretreatment) showed that CO oxidation activity was one order of magnitude lower for the Au/ $\text{TiO}_2$  catalysts. The catalyst deactivation was very slow, and studies showed that the catalyst could be successfully regenerated to regain initial activity. Diffuse reflectance infrared spectroscopy studies of CO on these supported catalysts are in excellent agreement with the infrared reflection absorption spectroscopy data obtained on model Au catalysts in our laboratory. The Au/ $\text{TiO}_2$  catalyst prepared by a temperature-programmed reduction–oxidation treatment showed high  $\text{CO}_2$  yield for the CO oxidation reaction in the presence of excess hydrogen. © 2002 Elsevier Science (USA)

**Key Words:** CO oxidation; Au/ $\text{TiO}_2$ ; PROX; stability; phosphine complex.

## 1. INTRODUCTION

CO oxidation is of considerable environmental concern, since even small exposures to CO (ppm) can be lethal. It is therefore of interest to develop highly active CO oxidation catalysts to remove trace amounts of CO. Historically, gold was considered to be inactive; however, recently Haruta and co-workers (1) showed that highly dispersed gold catalysts are extremely active for CO oxidation and exhibit high catalytic activity even at subambient temperatures. Following this work, there have been a number of investigations dealing with gold-based catalysts for CO oxidation (2–9) as

well as other reactions such as methane oxidation (10–12), propylene epoxidation (13, 14), hydrogenation (15–17), and  $\text{NO}_x$  reduction (18, 19).

The CO oxidation activity is strongly influenced by the catalyst preparation methods. Bamwenda *et al.* (20) observed that the CO oxidation activity of Au/ $\text{TiO}_2$  synthesized by the deposition–precipitation method was four orders of magnitude greater than that of Au/ $\text{TiO}_2$  synthesized by the photodeposition method. In general, coprecipitation, deposition–precipitation, and chemical vapor deposition methods produce highly dispersed gold catalysts (particle size < 5 nm) with high activity for CO oxidation (21). Although the wet-impregnation method usually yields inactive catalysts, studies by Vannice and co-workers showed that these catalysts could be activated by following specific reduction–oxidation treatment procedures (22). Recently, Iwasawa and co-workers obtained highly active CO oxidation catalysts by grafting Au–phosphine complexes ( $\text{AuL}_3\text{NO}_3$  or  $\text{Au}_9\text{L}_8(\text{NO}_3)_3$ ;  $\text{L} = \text{PPh}_3$ ) onto “as-precipitated”  $\text{Ti}(\text{OH})_4$  (4). In a series of papers (4, 23–27), the authors strongly emphasized that the “as-precipitated”  $\text{Ti}(\text{OH})_4$  was essential for obtaining highly dispersed active catalysts and that the use of a conventional  $\text{TiO}_2$  support resulted in an inactive CO oxidation catalyst (order of magnitude lower activity) with a particle size greater than 15 nm. We report here for the first time the successful synthesis of highly dispersed Au catalysts (< 5 nm) using a wet-impregnation method on a conventional  $\text{TiO}_2$  support. High-temperature reduction–oxidation pretreatment of  $[\text{Au}_6(\text{PPh}_3)_6](\text{BF}_4)_2/\text{TiO}_2$  resulted in highly dispersed gold catalysts with activities higher than those observed by Iwasawa and co-workers on the Au/ $\text{Ti}(\text{OH})_4$  systems (4). The effect of various pretreatment conditions on the CO oxidation activity was highlighted in this investigation. Along with the kinetics of CO oxidation, the catalyst was also tested for preferential CO oxidation (PROX) in the presence of hydrogen. PROX is of great interest in state-of-the-art low-temperature fuel cell systems, as trace amounts of CO are known to poison fuel cell electrodes (28–33). PROX can be effectively employed to remove trace amounts of CO from the hydrogen stream prior to its

<sup>1</sup> Present address: Chemistry Department, University of Missouri–Rolla, Rolla, MO 65401.

<sup>2</sup> To whom correspondence should be addressed. E-mail: [goodman@mail.chem.tamu.edu](mailto:goodman@mail.chem.tamu.edu).

introduction into the fuel cell. One of the most challenging problems faced by Au catalysts is stability and regeneration; this aspect has received little attention (34, 35). This paper includes an investigation dealing with catalyst stability and regeneration.

## 2. EXPERIMENTAL

### 2.1. Catalyst Synthesis

The supported gold catalyst was synthesized by grafting an  $[\text{Au}_6(\text{PPh}_3)_6](\text{BF}_4)_2$  complex onto  $\text{TiO}_2$ . The synthesis of  $[\text{Au}_6(\text{PPh}_3)_6](\text{BF}_4)_2$  is reported elsewhere (36–38). The complex was dissolved in  $\text{CH}_2\text{Cl}_2$  and deposited on  $\text{TiO}_2$  (Degussa) at room temperature to obtain a nominal gold loading of 1 wt% with respect to the support. Following this, the catalyst was mixed thoroughly for ca. 2 h at room temperature until the solvent had completely evaporated.  $\text{TiO}_2$  (Degussa P-25; surface area, 35–65  $\text{m}^2/\text{g}$ ) was calcined at 723 K for 4 h prior to the catalyst synthesis. The as-synthesized catalyst was then pretreated under different conditions prior to testing for catalytic activity. The following pretreatment methods were employed: (i) calcination in 1:2 air + He mixture at 673 K for 1 h (LTC); (ii) calcination in 1:2 air + He mixture at 773 K for 1 h (HTC); (iii) heating in 1:2  $\text{H}_2$  + He mixture at 773 K for 30 min, flushing with He for 10 min, and calcination in 1:2 air + He mixture for 30 min at 673 K (HTR/LTC); and (iv) calcination in 1:2 air + He mixture at 773 K for 30 min, flushing with He for 10 min, and heating in 1:2  $\text{H}_2$  + He mixture at 673 K for 30 min (HTC/LTR). After the pretreatment the sample was cooled to the desired reaction temperature and a ramp rate of 5 K/min was employed for sample heating.

### 2.2. Catalyst Characterization and Instrumental Techniques

**2.2.1. Transmission electron microscopy (TEM).** TEM micrographs of the supported Au catalysts were initially obtained using a Zeiss 10 C electron microscope (Electron Microscopy Center, Texas A&M University). To confirm the results, the TEM study was also conducted on a high-resolution JEOL 2010 microscope at the University of New Mexico. Essentially identical results were obtained on both microscopes. Samples after reaction were ultrasonically dispersed in ethanol/acetone and spread over perforated carbon grids. On the high-resolution microscope, several bright-field TEM micrographs of different portions of the sample were obtained at magnifications up to 400,000, whereas on the Zeiss 10 C the micrographs were obtained at magnifications up to 100,000. At least 100 particles were used to obtain a particle size distribution.

**2.2.2. X-ray photoelectron spectroscopy (XPS).** XPS was performed in an ion-pumped (300 L/s) Perkin–Elmer

PHI 560 system using a PHI 25–270AR double-pass cylindrical mirror analyzer. Survey scans were performed using a 100-eV pass energy; high-resolution scans were performed with a 50-eV pass energy. The signal from adventitious carbon at  $\text{BE} = 284.7$  eV for the C 1s level was used to correct for sample charging. Samples were mounted onto a  $1.0 \times 1.0 \times 0.1$  cm support using a double-sided tape (Scotch 3 M) attached to a probe and introduced into the UHV via a turbopumped antechamber. The support was attached to a probe that was differentially pumped using sliding seals. Curve fitting of the XPS data was performed using Peakfit Ver. 3.1 B (Jandel Scientific) software. Detailed information regarding the XPS instrument is available elsewhere (39).

**2.2.3. Diffuse reflectance infrared spectroscopy (DRIFTS).** The DRIFTS experiments were performed with a Perkin–Elmer Spectrum 2000 spectrometer equipped with a MCT detector and a DRIFTS (Harrick) cell used in a flow mode. The samples under investigation were treated *in situ* when pretreatment temperatures were less than 673 K; they were treated externally in a quartz reactor for treatment temperatures exceeding 673 K. The number of scans employed varied from 25 to 100 depending on the conditions and the sample employed. Background signals from gas-phase CO and  $\text{CO}_2$  were subtracted before the spectra were reported.

### 2.3. Catalyst Activity Tests

The activity tests were carried out in a conventional-flow reactor system consisting of a quartz reactor, a custom-built furnace, and an Omega temperature controller which could be used to ramp the temperature at the desired heating rate. The gas-analysis system consisted of a Varian 3700 gas chromatograph equipped with a thermal conductivity detector and a carbosphere column for gas separation. CO (research purity, Matheson),  $\text{O}_2$  (UHP, Matheson), and He (UHP, Matheson) were employed for the study. Preliminary partial dependence studies of CO and  $\text{O}_2$  on the CO oxidation activity revealed identical reaction orders for the HTR/LTC- and the HTC/LTR-treated samples. Detailed studies (similar to those in Ref. (22)) were carried out on the HTC/LTR-treated sample, under conditions where there was very little/no catalyst deactivation, with the conversion maintained below 20%. The catalytic activity for the different pretreatments was measured at a gas-hourly space velocity (GHSV) of 20,000  $\text{cm}^3/\text{g/h}$  and CO and  $\text{O}_2$  partial pressures of 3.67 kPa. The gas composition for the PROX reaction was  $\text{CO} : \text{O}_2 : \text{H}_2 : \text{He} = 1 : 2 : 50 : 25$  and the GHSV was 90,000  $\text{cm}^3/\text{g/h}$ . The gas-feed concentration was varied using Brooks mass flow controllers. The catalysts were used in a finely powdered state, and evaluation of the Weisz criterion (40) showed the absence of any mass-transfer-related problems. A carbon mass balance of  $\pm 3\%$  was obtained for the activity runs.

### 3. RESULTS

Figure 1a shows the TEM image of 1% Au/TiO<sub>2</sub> after the HTR/LTC treatment of the as-synthesized catalyst. It is apparent that the HTR/LTC procedure results in a high dispersion of gold particles on TiO<sub>2</sub>. A major fraction of the gold particles were in the range of 3–6 nm (shown in Fig. 1b) and exhibited an average particle size of 4.7 nm. It is noteworthy that the size of the gold particles did not exceed 8 nm. However, larger gold particles were observed after the HTC and HTC/LTR treatment procedures (Figs. 2a and 2b). In the case of HTC-pretreated catalysts (Fig. 2a), although the particle size varied from 3 to 12 nm, most of the particles were concentrated in the 7–9 nm region. In contrast, a larger range of particle size distribution (with higher density in the 5–11 nm region) was observed subsequent to

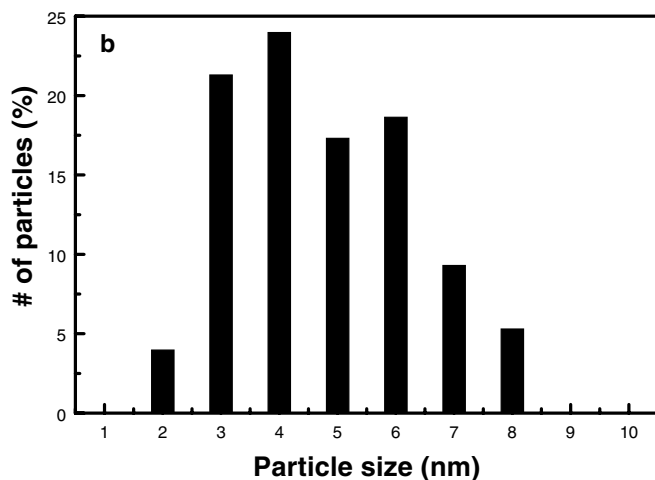
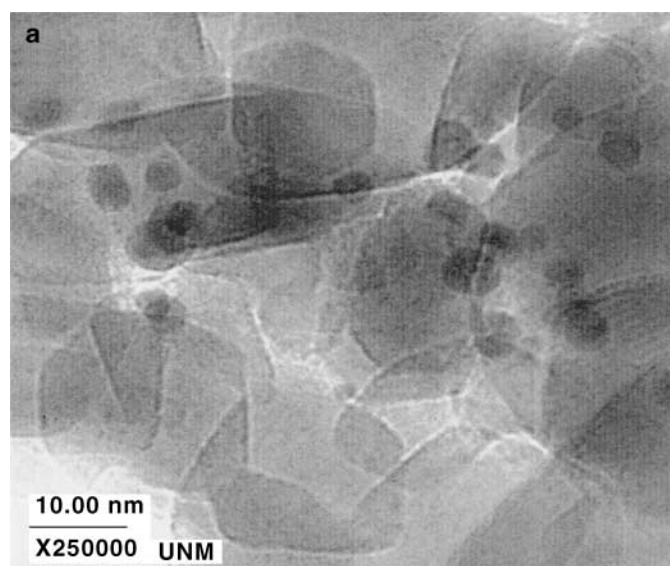


FIG. 1. (a) TEM image and (b) particle size distribution for the HTR/LTC-treated Au/TiO<sub>2</sub> sample.

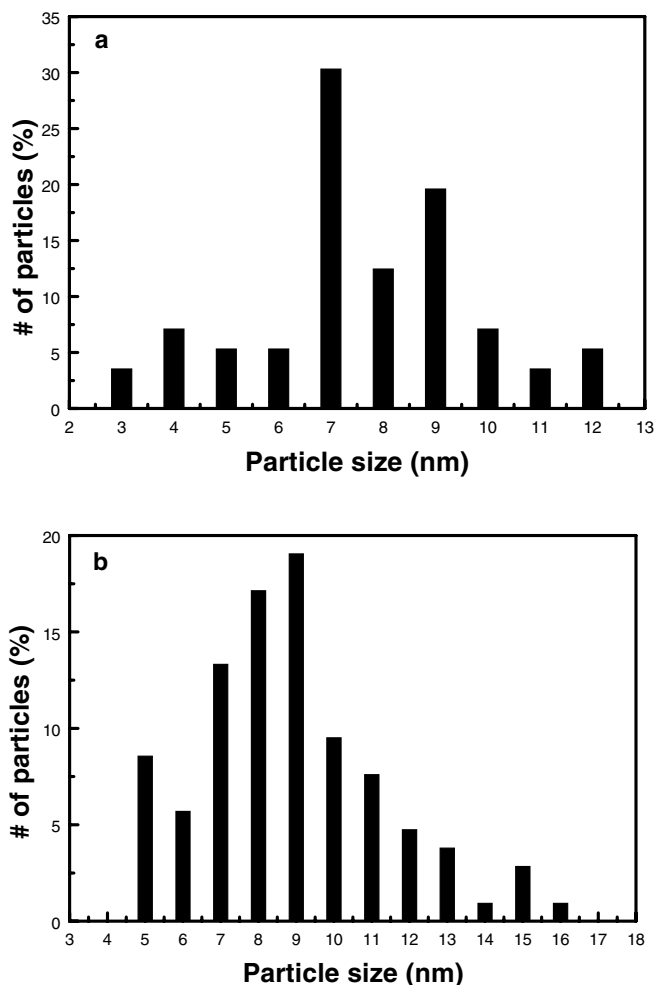


FIG. 2. Particle size distribution for the (a) HTC-treated and (b) HTC/LTR-treated Au/TiO<sub>2</sub> catalyst.

the HTC/LTR treatment procedures. The average particle sizes were estimated to be 7.9 and 8.5 nm, respectively, for the HTC- and HTC/LTR-treated samples.

The XP spectra of Au 4*f* and P 2*p* levels under various treatment conditions are shown in Figs. 3a and 3b, respectively. Similar to the work of Iwasawa and co-workers (26), a shift from a higher binding energy (84.7 eV) for as-synthesized Au/TiO<sub>2</sub> catalysts to a lower (ca. 83.6–83.9 eV) binding energy for catalysts treated at high temperatures (>673 K) was observed for the Au 4*f*<sub>7/2</sub> level. This is in good agreement with the transformation of the Au-phosphine complex to metallic gold particles as reported in the literature (26). The absence of appreciable binding energy shifts for the HTC, HTR/LTC, and HTC/LTR treatment conditions precludes any appreciable electronic structural change for the gold particles due to the different pretreatment procedures. For the as-synthesized samples, two peaks due to phosphorous were observed at 131.6 and 135.3 eV, respectively (Fig. 3b). The higher binding energy

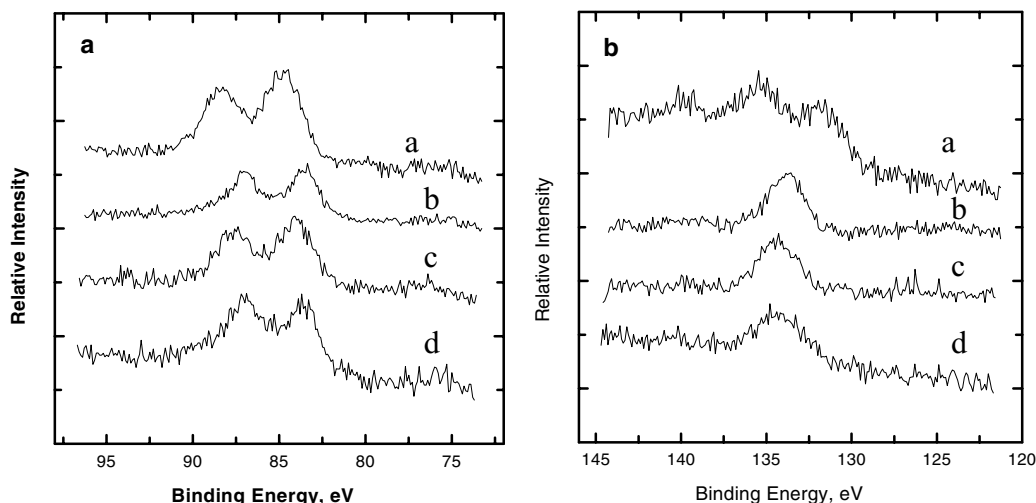


FIG. 3. XPS spectra of the (a) Au 4f and (b) P 2p for the Au/TiO<sub>2</sub> catalysts after a, no pretreatment; b, HTC; c, HTR/LTC; and d, HTC/LTR treatments.

feature disappeared after the high-temperature treatments ( $\geq 673$  K), whereas the peak at 131.6 eV shifted to the region 133.8–134.2 eV. Similarly to a previous study (26), this shift is attributed to the oxidation of the phosphine species during the high-temperature treatments.

Figure 4 shows the effect of the CO oxidation catalytic activity (27.5 Torr CO and 27.5 Torr O<sub>2</sub>) of the Au/TiO<sub>2</sub> sample as a function of different pretreatment procedures. The as-synthesized sample showed no catalytic activity at temperatures below 373 K (not shown in the figure). A difference in CO conversion of more than an order of magnitude was observed at room temperature (293 K) for the LTC- and the HTR/LTC-pretreated catalysts. The order of the

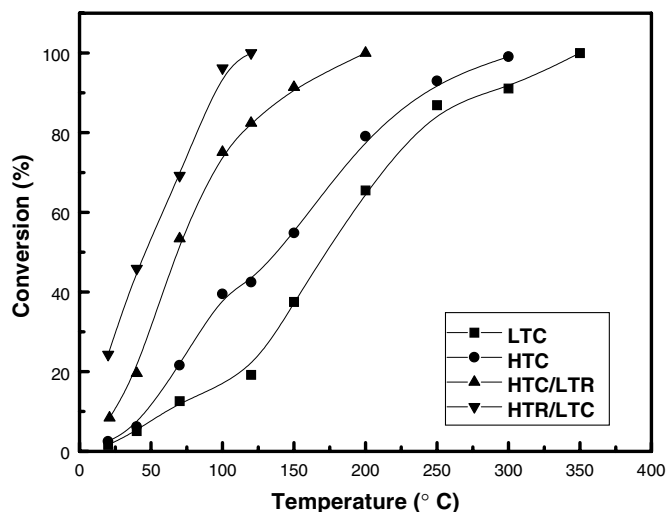


FIG. 4. Effect of different pretreatments on the CO conversion as a function of temperature (GHSV = 20,000 cm<sup>3</sup>/g/h;  $P_{\text{CO}} = 3.67$  kPa and  $P_{\text{O}_2} = 3.67$  kPa).

catalytic activity for the different pretreatment conditions was  $\text{HTR/LTC} \gg \text{HTC/LTR} > \text{HTC} > \text{LTC}$ . While 100% CO conversion was achieved at 393 K for the HTR/LTC-treated catalyst, complete CO conversions were obtained only at 623 K for the LTC sample. Table 1 compares the CO oxidation catalytic activities for Au/TiO<sub>2</sub> samples synthesized by the various procedures. The HTR/LTC catalyst clearly shows CO oxidation activity comparable to that of the most active Au/TiO<sub>2</sub> catalysts reported in the literature.

The catalyst stability/regeneration investigation on a HTR/LTC-treated sample is depicted in Fig. 5. In these studies, a 1 : 2 CO/Oxygen ratio was used to simulate harsh

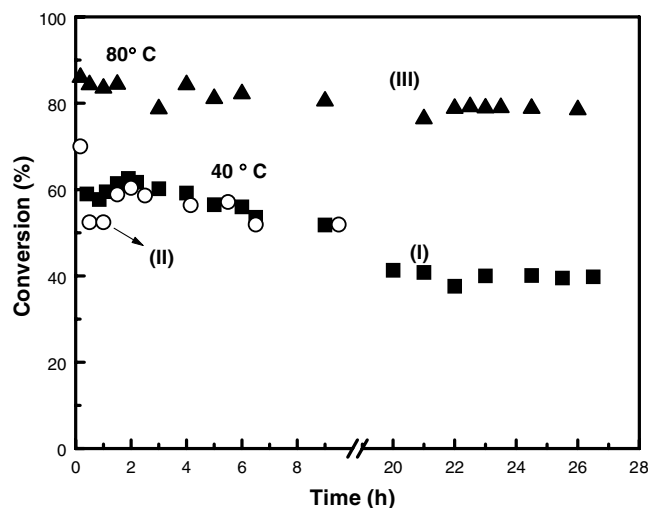


FIG. 5. Time-on-stream profile of the Au/TiO<sub>2</sub> sample after I, fresh HTR/LTC treatment sample ( $T_{\text{rxn}} = 313$  K); II, after first regeneration by HTR/LTC treatment ( $T_{\text{rxn}} = 313$  K); and III, after second regeneration by HTR/LTC treatment ( $T_{\text{rxn}} = 353$  K). (GHSV = 20,000 cm<sup>3</sup>/g/h;  $P_{\text{CO}} = 3.67$  kPa and  $P_{\text{O}_2} = 7.34$  kPa).

operating conditions; it is known from the literature that long exposures to air cause sintering of the gold particles and thereby deactivation (7). Both the pretreatment and the regeneration treatments involved HTR/LTC treatments. After initial CO oxidation (27 h) at 313 K (profile I), the catalyst was regenerated and again tested for activity at 313 K (profile II). Following this, the catalyst was again regenerated and CO oxidation was carried out at 353 K (Reaction III). The deactivation rate for Reaction I was relatively small for the initial 9 h and dropped from 59 to 41% over a period of 20 h. The activity remained constant after this period until the reaction was stopped (27 h). Following regeneration, the initial activity was reobtained in II and a profile similar to that of I was obtained, indicating excellent regeneration of the catalyst. After the second regeneration, the catalytic activity was observed to decrease from ca. 87 to ca. 80% (reaction temperature, 353 K) after 21 h, subsequent to which stabilized CO oxidation conversion was obtained.

Figure 6 shows the partial pressure dependence of the CO oxidation reaction on CO and O<sub>2</sub> at 293 K. For these studies, the partial pressure of either CO or O<sub>2</sub> was maintained at 27.5 Torr while the other was varied. The slopes of the linear graphs obtained by plotting the CO turnover frequency (TOF) versus pressure in logarithmic form were used to estimate the order of the reaction. The order of the CO oxidation reaction was found to be 0.2 with respect to CO and 0.46 with respect to O<sub>2</sub>. These studies are in excellent agreement with a recent study on similar systems, where the reaction orders were found to be 0.25 and 0.41 for CO and O<sub>2</sub>, respectively (24). On Au/TiO<sub>2</sub> catalysts prepared by the wet-impregnation method, Lin *et al.* (22) observed reaction orders of 0.24 (*P*: 17–187 Torr) and 0.4 for CO and O<sub>2</sub>, respectively, at 313 K. Their studies indicate

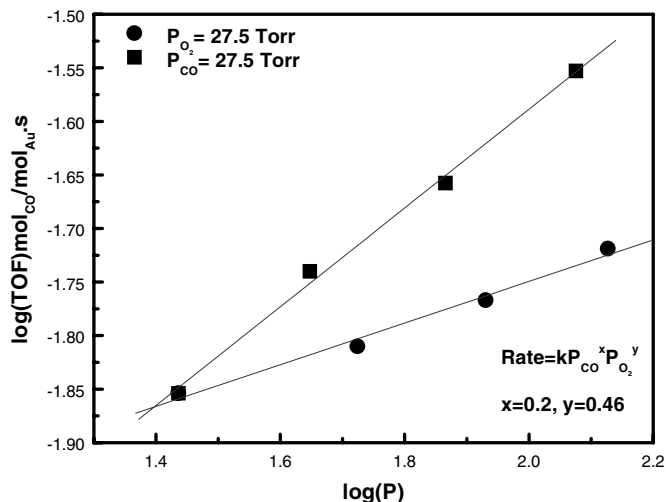


FIG. 6. Partial pressure dependence of CO (at constant  $P_{O_2} = 27.5$  Torr) and O<sub>2</sub> (at constant  $P_{CO} = 3.67$  kPa) on the CO oxidation activity at 293 K (HTR/LTR-treated sample: GHSV = 20,000 cm<sup>3</sup>/g/h).

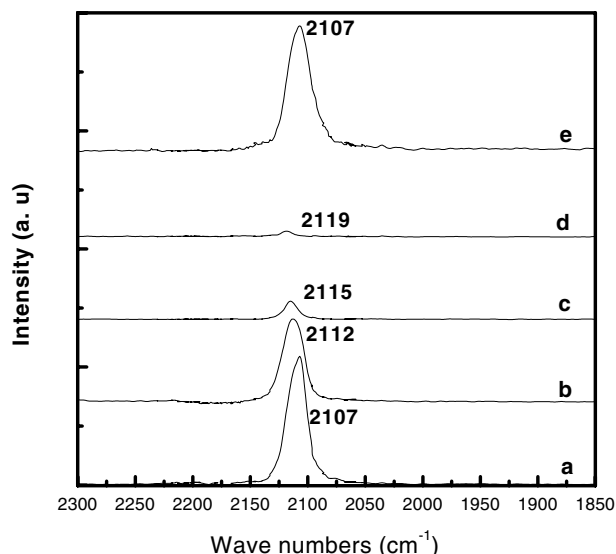


FIG. 7. DRIFT spectra of CO surface species on the HTR/LTC-treated sample at 293 K (a) under 5% CO in He after 10 min, (b) under 5% CO and 5% O<sub>2</sub> in He after 10 min, (c) 5 min after stopping CO and O<sub>2</sub>, (d) 12 min after stopping CO and O<sub>2</sub>, and (e) 8 min after reintroducing 5% CO in the He stream.

that the CO reaction orders are dependent on temperature and pressure.

The DRIFTS spectra shown in Fig. 7 were obtained under different reactant feed compositions on the HTR/LTC-treated Au/TiO<sub>2</sub> sample. Ten minutes after the introduction of CO, an adsorption feature due to CO (shown in Fig. 7a) appeared at 2107 cm<sup>-1</sup> and is attributed to CO adsorption on gold sites (consistent with previous literature data (2)). Apart from this, low-intensity nonresolved broad features (not shown in the figure) were observed in the carbonate/carboxylate region (1200–1700 cm<sup>-1</sup>). In good correspondence to the work by Bollinger and Vannice (2), no peak was observed at ~2183 cm<sup>-1</sup> on the Au/TiO<sub>2</sub> sample, indicating the absence of adsorbed CO on TiO<sub>2</sub>. The introduction of air into the CO + He mixture resulted in a peak shift of the adsorbed CO to 2112 cm<sup>-1</sup>. Along with this an additional intense and broad feature from gas-phase CO<sub>2</sub> was observed (the gas-phase signal has not been shown). The peak shift of the CO band to higher binding energy is consistent with the decrease of the CO coverage on Au and corroborates recent work in our group on CO probed by infrared reflection absorption spectroscopy (IRAS) on the Au(110) surface (41). Spectra c and d, which were obtained after stopping CO and air, showed a decreasing CO coverage on the gold surface with time and indicated weak chemisorption of CO on gold (consistent with literature reports (2, 42)). In line with the earlier trend, the peaks shifted to higher binding energies with decreasing CO coverage. After the peak due to CO adsorption had completely disappeared, CO was again introduced into the He stream

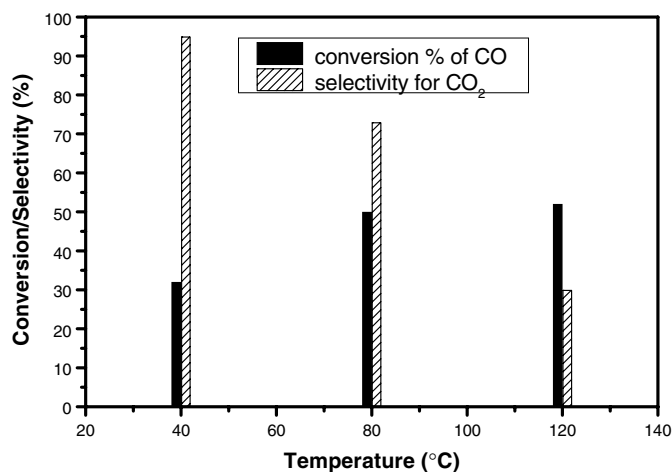


FIG. 8. Conversion/selectivity for the PROX reaction on the HTR/LTC-treated sample as a function of reaction temperature (GHSV = 90,000 cm<sup>3</sup>/g/h; CO : H<sub>2</sub> : O<sub>2</sub> : He = 1 : 50 : 2 : 25).

and spectrum e was obtained. This procedure resulted in a peak at the same position as that obtained in spectrum a (2107 cm<sup>-1</sup>), showing the reproducibility of the peak shifts with CO surface coverage.

The results obtained from the preferential CO oxidation studies on the HTR/LTC-treated Au/TiO<sub>2</sub> in the presence of excess hydrogen are shown in Fig. 8. The CO conversion increased with an increase in temperature, whereas the selectivity decreased. The Au/TiO<sub>2</sub> catalyst showed an extremely high propensity to oxidize CO preferentially at 313 K (95% selectivity for CO oxidation). It should be noted that while an increase in temperature from 353 to 393 K only marginally increased the conversion, it resulted in a drastic decrease (73 to 30%) in the CO oxidation selectivity.

#### 4. DISCUSSION

Gold catalysts have received wide attention in recent years due to their exceptionally high CO oxidation activity. In general, high catalytic activity has been observed only on highly dispersed Au catalysts (particle size <5 nm). The study by Lin and Vannice (22) is an exception in that reasonably high CO oxidation catalytic activity was observed on Au/TiO<sub>2</sub> (average particle size of 30 nm) after a sequential reduction–oxidation–reduction treatment. Catalyst preparation methods such as deposition–precipitation, coprecipitation, and chemical vapor deposition have been regularly used to obtain Au catalysts with average particle sizes of less than 5 nm. Recent studies by Iwasawa and co-workers have shown that highly dispersed Au catalysts can also be obtained by the interaction of an Au–phosphine complex with as-precipitated wet metal hydroxide supports (4). In particular, the Au/Ti(OH)<sub>4</sub> catalyst was obtained by grafting Au(PPh<sub>3</sub>)(NO<sub>3</sub>) onto the as-precipitated Ti(OH)<sub>4</sub>

followed by a temperature-programmed (4 K/min) calcination treatment; Ti(OH)<sub>4</sub> was prepared by the hydrolysis of titanium–tetraisopropoxide with sodium carbonate and further washed and filtered as explained in Ref. (26). Under Yuan *et al.*'s experimental conditions, the freshly prepared Ti(OH)<sub>4</sub> was found to be essential for the synthesis of highly dispersed Au catalysts; conventional TiO<sub>2</sub> and commercial Ti(OH)<sub>4</sub> were found to be inefficient for the successful synthesis (4, 26).

The present study has demonstrated the successful synthesis (Figs. 1a and 1b) of highly dispersed Au catalysts (<5 nm) by the temperature-programmed reduction–calcination (HTR/LTC) of Au<sub>6</sub>(PPh<sub>3</sub>)<sub>6</sub>(BF<sub>4</sub>)<sub>2</sub> with a conventional TiO<sub>2</sub> support (Degussa P-25), as predicted by theoretical calculations (43). Similarly, recent STM studies (44) in our laboratory have revealed the presence of highly dispersed Au (<5 nm) on a TiO<sub>2</sub> support after a wet chemistry deposition of Au<sub>6</sub>(PPh<sub>3</sub>)<sub>6</sub>(BF<sub>4</sub>)<sub>2</sub> on planar TiO<sub>2</sub> (110). In contrast, Iwasawa and co-workers observed an average particle size of ca. 30 nm after the temperature-programmed calcination (heating rate: 4 K/min, 4 h in air) of Au(PPh<sub>3</sub>)(NO<sub>3</sub>) and the conventional TiO<sub>2</sub> (Degussa P-25 support). Interestingly, the high-temperature calcination (HTC) treatment employed in our study also resulted in a catalyst with an average particle size of only ca. 8 nm. The reason for the above is not clearly understood at this point; however, it should be noted that the solvents for the phosphine complex were different (CH<sub>2</sub>Cl<sub>2</sub> in our study as opposed to acetone in the study by Iwasawa and co-workers). Iwasawa and co-workers (27) emphasized the importance of both the state of the support surface and the choice of the Au complex in the synthesis process. The solvents, owing to their difference in polarity, may alter support surfaces in different ways and hence modify the cluster–support interaction. That the HTR/LTC treatment plays a decisive role in stabilizing the Au clusters on TiO<sub>2</sub> is apparent from our studies.

As discussed earlier, the CO oxidation activity for the HTR/LTC sample was comparable to that of the most active Au/TiO<sub>2</sub> catalysts reported in the literature (Table 1). The CO oxidation activity of the HTR/LTC-treated sample had ca. 100 times greater CO oxidation activity than that of the catalysts (calcined at 673 K) prepared from the Au–phosphine complex on the conventional Degussa support by Iwasawa and co-workers (26). More importantly, the HTR/LTC-treated sample showed ca. five times greater activity than that of the most active Au/Ti(OH)<sub>4</sub> samples employed in Refs. (4, 26). It should be noted (from Table 1) that different partial pressures of CO and O<sub>2</sub> were employed in the two studies. This, however, does not pose problems for comparison, since the partial pressure dependence of the reactants on the CO oxidation activity is similar for both studies (see Results). Calculations indicate that a direct comparison (from Table 1) of the catalysts is valid in this case, as the greater activity expected due to the

TABLE 1

Comparison of CO Oxidation Rates on Au/TiO<sub>2</sub> Catalysts Prepared by Different Methods

Au precursor	Catalyst	Preparation methods <sup>a</sup>	$d_{\text{Au}}$ (nm)	$P_{\text{CO}}$ (kPa)	$P_{\text{O}_2}$ (kPa)	$T$ (K)	$E_a$ (kJ/mol)	Rate CO (mmol/s/g <sub>Au</sub> )	References
HAuCl <sub>4</sub>	2.3% Au/TiO <sub>2</sub>	DP	2.5	1	20	300	20	0.2	(20)
HAuCl <sub>4</sub>	3.1% Au/TiO <sub>2</sub>	DP	2.9	1	20	300	27	0.6	(20)
HAuCl <sub>4</sub>	1% Au/TiO <sub>2</sub>	FD	4.6	1	20	300	56	$2 \times 10^{-5}$	(20)
HAuCl <sub>4</sub>	1% Au/TiO <sub>2</sub>	IMP	nr	1	20	300	58	$2 \times 10^{-5}$	(20)
HAuCl <sub>4</sub>	2.3% Au/TiO <sub>2</sub>	IMP	30	5	4.8	313	13	0.05 <sup>b</sup>	(22)
Me <sub>2</sub> Au(acac)	4.6% Au/TiO <sub>2</sub>	CVD	~2.9	1	20	262	nr	0.05 <sup>c</sup>	(3)
Me <sub>2</sub> Au(acac)	2.4% Au/TiO <sub>2</sub>	CVD	nr	1	20	293	nr	0.06 <sup>d</sup>	(3)
HAuCl <sub>4</sub>	1.7% Au/TiO <sub>2</sub>	AuC	2	0.25	0.25	300	nr	0.01	(9)
AuPPh <sub>3</sub> NO <sub>3</sub>	3% Au/Ti(OH) <sub>4</sub>	IOH	3	1	20	300	nr	0.05	(26)
AuPPh <sub>3</sub> NO <sub>3</sub>	3% Au/TiO <sub>2</sub>	IMP	30	1	20	313	12	$6 \times 10^{-3}$	(26)
Au <sub>6</sub> (PPh <sub>3</sub> ) <sub>6</sub> (BF <sub>4</sub> ) <sub>2</sub>	1% Au/TiO <sub>2</sub>	IMP	4.7	3.67	9	293	16.3	0.3 <sup>e</sup>	<sup>f</sup>

<sup>a</sup> Abbreviations used: DP, deposition–precipitation; FD, photodecomposition; IMP, impregnation of oxides; IOH, impregnation of as-precipitated hydroxide; CVD, chemical vapor deposition; nr, not reported.

<sup>b</sup> HTR/C/ITR.

<sup>c</sup> amorphous TiO<sub>2</sub>.

<sup>d</sup> anatase TiO<sub>2</sub>.

<sup>e</sup> HTR/LTC.

<sup>f</sup> Present work.

high partial pressures of CO used in our work is essentially compensated for by the larger O<sub>2</sub> partial pressures used in the study by Iwasawa and co-workers. The higher activity of our catalyst may be tentatively attributed to the difference in preparation procedure. The beneficial effect of the reduction–oxidation treatment observed in this study is similar to that observed by Lin *et al.* (22) on Au/TiO<sub>2</sub> catalysts prepared by the wet-impregnation method, wherein the highest activity (22) was observed after the following sequence: high-temperature reduction at 773 K followed by calcination at 673 K and finally low-temperature reduction at 473 K (HTR/C/ITR). The authors strongly emphasized the high-temperature reduction requirement to obtain high CO oxidation catalytic activity. Their studies revealed that a HTR treatment induced a low CO oxidation activity in TiO<sub>2</sub>, which was otherwise totally inactive for CO oxidation (22). However, it is clear that the large increase in activity after the HTR/LTC treatment cannot be explained by the contribution from the support alone. According to the literature, a high-temperature reduction treatment causes some transformation from the anatase form to the rutile form (45). Based on our results and those in the literature, it may be speculated that the HTR/LTC pretreatment modifies the TiO<sub>2</sub> support so that there is an optimized interaction between Au (obtained from [Au<sub>6</sub>(PPh<sub>3</sub>)<sub>6</sub>](BF<sub>4</sub>)<sub>2</sub>] complex) and TiO<sub>2</sub>; this leads to a higher dispersion and an enhanced CO oxidation activity. Further studies are, however, required to provide a clearer definitive view of this process. The CO oxidation activity observed in our work was much higher than that found in the study by Lin *et al.* (22), because of the enhanced Au dispersion (average particle size = 4.7 nm) in our case as opposed to that in their

work (average particle size = 30 nm). The difference in dispersion is attributed to the different decomposition behavior of the Au precursors used in the two studies; AuCl<sub>3</sub> was used in their investigation while [Au<sub>6</sub>(PPh<sub>3</sub>)<sub>6</sub>](BF<sub>4</sub>)<sub>2</sub> was employed in this study.

The HTR/LTC-treated sample showed very slow initial catalyst deactivation at 313 K, followed by stable conversions for many hours (Fig. 5, profile I). In contrast, studies on model catalyst systems (46) and catalysts synthesized by the conventional deposition–precipitation method (47) showed rapid deactivation during CO oxidation at above ambient temperatures. The deactivation was also found to be more rapid in Au/TiO<sub>2</sub> catalysts synthesized by the conventional wet-impregnation method (22). Most importantly, our studies have shown that the HTR/LTC sample could be successfully regenerated (as seen from the similarity of the time-on-stream profile to that of the fresh catalyst after regeneration (profile II, Fig. 5)) by a subsequent HTR/LTC treatment. Even after the second regeneration (profile III), when the CO oxidation reaction was carried out at 353 K, the catalyst followed a trend similar to that of the fresh sample: very slow initial deactivation followed by stable conversions. These investigations, which were performed over periods longer than 24 h, clearly show that the HTR/LTC-treated sample is stable and can easily be regenerated. The observed high stability may be attributed to the stabilization effect of the HTR/LTC treatment of the Au clusters on the TiO<sub>2</sub> surface.

The kinetics experiments (Fig. 6) show that the reaction orders for CO oxidation on our Au/TiO<sub>2</sub> catalyst are 0.2 and 0.46 for CO and O<sub>2</sub>, respectively. These agree very well with the values obtained by Iwasawa and co-workers

(24) on Au/Ti(OH)<sub>4</sub>, wherein they proposed a Langmuir–Hinshelwood model which involved the reaction of adsorbed CO molecules (Au surface) with O<sub>2</sub> (adsorbed on oxygen vacancies of the support) as the rate-limiting step. The activation energy (16.3 kcal/mol) obtained in this study for the HTR/LTC sample lies within the range of values (12–21 kcal/mol) observed by Iwasawa and co-workers (23) on the catalysts synthesized from Au–phosphine complexes and TiO<sub>2</sub>. Our DRIFTS studies show weak CO chemisorption on the Au surface and indicate a blue shift of the CO band at lower CO coverages. The position of the CO band (DRIFTS) and the XPS (Au 4f) provide evidence that Au is present in the metallic form after the HTR/LTC treatment. The XPS also reveals the presence of an oxidized phosphorus species on the surface; however, at this point, the role and nature of this species are unknown.

The main requirement for an effective PROX catalyst is high CO oxidation activity coupled with low hydrogen oxidation activity. CO oxidation in the presence of excess hydrogen (Fig. 8) shows promising results for the HTR/LTC treated sample. A high selectivity of ca. 73% for CO<sub>2</sub> was obtained at a high CO oxidation rate of 0.6 mmol/s/g<sub>Au</sub> (CO:H<sub>2</sub>:O<sub>2</sub> = 1:50:2) at 353 K, the approximate operating temperature of a PEM fuel cell. Comparison with previous work (Au/MnO<sub>x</sub>: ~0.2 mmol/s/g<sub>Au</sub> at 353 K (48) and Au/Al<sub>2</sub>O<sub>3</sub>: ~0.3–1.7 mmol/s/g<sub>Au</sub> at 363 K (32) indicates comparable activities for CO oxidation for the PROX reaction. Operation temperatures above 373 K result only in a marginal increase in the CO oxidation activity while greatly decreasing the selectivity for the desired CO<sub>2</sub> product, thus implying a favorable pathway for hydrogen oxidation over CO oxidation at higher temperatures. These results are similar to those of previous studies (6, 29), which show that highly dispersed Au particles are more active for CO oxidation as compared to hydrogen oxidation at low temperatures, while larger Au particles are more active for hydrogen oxidation.

## 5. CONCLUSION

Highly dispersed and active Au catalysts were synthesized by wet impregnation of [Au<sub>6</sub>(PPh<sub>3</sub>)<sub>6</sub>](BF<sub>4</sub>)<sub>2</sub> on a conventional TiO<sub>2</sub> support. The pretreatment conditions played a crucial role in defining catalyst dispersion and activity. The HTC/LTR treatment produced not only extremely active CO oxidation catalysts but also highly stable catalysts that could be easily regenerated. Characterization studies showed the presence of metallic Au on the surface along with some oxidized phosphorus species after the HTR/LTC treatment. DRIFTS experiments revealed weak chemisorption of CO on the metallic Au particles, with a blue shift of the CO band at decreasing CO coverages. The HTR/LTC-treated sample was found to be a promising catalyst for PROX reactions.

## ACKNOWLEDGMENTS

We acknowledge with pleasure the support of this work by the Department of Energy, Office of Basic Energy Sciences, Division of Chemical Sciences. We are grateful to Professor J. H. Lunsford for giving us access to the DRIFTS setup, to Professor P. R. Sharp (University of Missouri at Columbia) for supplying us with the gold complex for these studies, and to D. C. Meier for helpful discussions on the DRIFTS data. TVC gratefully acknowledges the Link Foundation for the Link Energy Fellowship. CCC gratefully acknowledges support from the Associated Western Universities, Inc., and Pacific Northwest National Laboratories operated by Battelle Memorial.

## REFERENCES

1. Haruta, M., Tsubota, S., Kobayashi, T., Kageyama, H., Genet, M. J., and Delmon, B., *J. Catal.* **144**, 175 (1993).
2. Bollinger, M. A., and Vannice, M. A., *Appl. Catal. B* **8**, 417 (1996).
3. Okumura, M., Tanaka, K., Ueda, A., and Haruta, M., *Solid State Ionics* **95**, 143 (1997).
4. Yuan, Y., Kozlova, A. P., Akasura, K., Wan, H., Tsai, K., and Iwasawa, Y., *J. Catal.* **170**, 191 (1997).
5. Tsubota, S., Nakamura, T., Tanaka, K., and Haruta, M., *Catal. Lett.* **56**, 131 (1998).
6. Okamura, M., Nakamura, S., Tsubota, S., Nakamura, T., Azuma, M., and Haruta, M., *Catal. Lett.* **51**, 53 (1998).
7. Valden, M., Lai, X., and Goodman, D. W., *Science* **281**, 1647 (1998).
8. Griesel, R. J. H., and Nieuwenhuys, B. E., *J. Catal.* **199**, 48 (2001).
9. Grunwaldt, J.-D., Kiener, C., Wogerbauer, C., and Baiker, A., *J. Catal.* **181**, 223 (1999).
10. Waters, R. D., Weimer, J. J., and Smith, J. E., *Catal. Lett.* **30**, 181 (1995).
11. Griesel, R. J. H., Kooyman, P. J., and Nieuwenhuys, B. E., *J. Catal.* **191**, 430 (2000).
12. Choudhary, T. V., Banerjee, S., and Choudhary, V. R., Submitted for publication.
13. Hayashi, T., Tanaka, K., and Haruta, M., *J. Catal.* **178**, 566 (1998).
14. Strangland, E. E., Stavens, K. B., Andres, R. P., and Delgass, W. N., *J. Catal.* **191**, 332 (2000).
15. Sakurai, H., and Haruta, M., *Appl. Catal. A* **127**, 93 (1995).
16. Jia, J., Haraki, K., Kondo, J. N., Domen, K., and Tamaru, K., *J. Phys. Chem. B* **104**, 11,153 (2000).
17. Choudhary, T. V., Sivadinarayana, C., and Goodman, D. W., In preparation.
18. Salama, T. M., Ohnishi, Y., and Ichikawa, M., *J. Chem. Soc., Faraday Trans.* **92**, 301 (1996).
19. Salama, T. M., Ohnishi, R., and Ichikawa, M., *Chem. Commun.* 105 (1997).
20. Bamwenda, G. R., Tsubota, S., Nakamura, T., and Haruta, M., *Catal. Lett.* **44**, 83 (1997).
21. Bond, G. C., and Thompson, D. T., *Catal. Rev.-Sci. Eng.* **41**, 319 (1999).
22. Lin, S. D., Bollinger, M., and Vannice, M. A., *Catal. Lett.* **17**, 245 (1993).
23. Yuan, Y., Akasura, K., Wan, H., Tsai, K., and Iwasawa, Y., *Catal. Lett.* **42**, 15 (1996).
24. Liu, H., Kozlov, A., Kozlova, A. P., Shido, T., Akasura, K., and Iwasawa, Y., *J. Catal.* **185**, 252 (1999).
25. Yuan, Y., Akasura, K., Wan, H., Tsai, K., and Iwasawa, Y., *Chem. Lett.* 755 (1996).
26. Yuan, Y., Akasura, K., Kozlova, A. P., Wan, H., Tsai, K., and Iwasawa, Y., *Catal. Today* **44**, 333 (1998).
27. Kozlov, A., Kozlova, A. P., Liu, H., and Iwasawa, Y., *Appl. Catal. A* **182**, 9 (1999).
28. Choudhary, T. V., and Goodman, D. W., *Catal. Lett.* **59**, 93 (1999).
29. Griesel, R. J. H., and Nieuwenhuys, B. E., *J. Catal.* **199**, 48 (2001).



30. Choudhary, T. V., Sivadinarayana, C., and Goodman, D. W., *Catal. Lett.* **72**, 197 (2001).
31. Kahlich, M. J., Gasteiger, H. A., and Behm, R. J., *J. Catal.* **182**, 430 (1999).
32. Bethke, G. K., and Kung, H. H., *Appl. Catal. A* **194**, 43 (2000).
33. Choudhary, T. V., and Goodman, D. W., *J. Catal.* **192**, 316 (2000).
34. Gardner, S. D., Hoflund, G. B., Upchurch, B. T., Schryer, D. R., Kielen, E. J., and Schryer, J., *J. Catal.* **129**, 114 (1991).
35. Hutchings, G. J., Siddiqui, M. R. H., Burrows, A., Kiely, C. J., and Whyman, R., *J. Chem. Soc., Faraday Trans.* **93**, 187 (1997).
36. Ramamoorthy, V., Wu, Z., Yi, Y., and Sharp, P. R., *J. Am. Chem. Soc.* **114**, 1526 (1992).
37. Dyson, P. J., and Mingos, D. M. P., "Gold: Progress in Chemistry, Biochemistry and Technology" (H. Schmidbaur, Ed.), pp. 511–556. Wiley, New York, 1999.
38. Flint, B. W., Yang, Y., and Sharp, P. R., *Inorg. Chem.* **39**, 602 (2000).
39. Choudhary, T. V., Sivadinarayana, C., Chusuei, C., Klinghoffer, A., and Goodman, D. W., *J. Catal.* **199**, 9 (2001).
40. Weisz, P. B., *Chem. Eng. Prog. Series* **55**, 29 (1959).
41. Meier, D. C., Bukhtiyarov, V., and Goodman, D. W., In preparation.
42. Grunwaldt, J.-D., Maciejewski, M., Becker, O. S., Fabrizioli, P., and Baiker, A., *J. Catal.* **186**, 458 (1999).
43. Omary, M. A., Raevashdeh-Omary, M. A., Chusuei, C. C., Fackler, J. P., Jr., and Bagus, P. S., *J. Chem. Phys.* **114**, 10695 (2001).
44. Chusuei, C., Lai, X., Davis, K., Bowers, E., Fackler, J. P., Jr., and Goodman, D. W., *Langmuir* **17**, 4113 (2001).
45. Haller, G. L., and Resasco, D. E., *Adv. Catal.* **36**, 173 (1989).
46. Valden, M., Pak, S., Lai, X., and Goodman, D. W., *Catal. Lett.* **56**, 7 (1998).
47. Choudhary, T. V., Sivadinarayana, C., and Goodman, D. W., Unpublished work.
48. Sanchez, R. M. T., Ueda, A., Tanaka, K., and Haruta, M., *J. Catal.* **168**, 125 (1997).